

# Full and approximated NLO predictions for like-sign W-boson scattering at the LHC

---

**Stefan Dittmaier,<sup>a,\*</sup> Christopher Schwan<sup>b</sup> and Ramon Winterhalder<sup>c</sup>**

<sup>a</sup>*Physikalisches Institut, Albert-Ludwigs-Universität Freiburg,  
Hermann-Herder-Straße 3, 79104 Freiburg, Germany*

<sup>b</sup>*Institut für Theoretische Physik und Astrophysik, Universität Würzburg,  
Emil-Hilb-Weg 22, 97074 Würzburg, Germany*

<sup>c</sup>*Centre for Cosmology, Particle Physics and Phenomenology (CP3),  
Université catholique de Louvain, Chemin du Cyclotron 2, B-1348 Louvain-la-Neuve, Belgium  
E-mail: [stefan.dittmaier@physik.uni-freiburg.de](mailto:stefan.dittmaier@physik.uni-freiburg.de),  
[christopher.schwan@physik.uni-wuerzburg.de](mailto:christopher.schwan@physik.uni-wuerzburg.de),  
[ramon.winterhalder@uclouvain.be](mailto:ramon.winterhalder@uclouvain.be)*

We report on a recent calculation of next-to-leading-order (NLO) QCD and electroweak corrections to like-sign W-boson scattering at the Large Hadron Collider, including all partonic channels and W-boson decays in the process  $pp \rightarrow e^+ \nu_e \mu^+ \nu_\mu jj + X$ . The calculation is implemented in the Monte Carlo integrator `BONSAY` and comprises the full tower of NLO contributions of the orders  $\alpha_s^3 \alpha^4$ ,  $\alpha_s^2 \alpha^5$ ,  $\alpha_s \alpha^6$ , and  $\alpha^7$ . Our numerical results confirm and extend previous results, in particular the occurrence of large purely electroweak corrections of the order of  $\sim -12\%$  for integrated cross sections, which get even larger in distributions. We construct a *VBS approximation* for the NLO prediction based on partonic channels and gauge-invariant (sub)matrix elements potentially containing the vector-boson scattering (VBS) subprocess and on resonance expansions of the W decays. The VBS approximation reproduces the full NLO predictions within  $\lesssim 1.5\%$  in the most important regions of phase space. Moreover, we discuss results from different versions of *effective vector-boson approximations* at leading order, based on the collinear emission of W bosons of incoming (anti)quarks. However, owing to the only mild collinear enhancement and the design of VBS analysis cuts, the quality of this approximation turns out to be only qualitative at the LHC.

*Loops and Legs in Quantum Field Theory (LL2024)*  
14-19, April, 2024  
Wittenberg, Germany

---

\*Speaker

## 1. Introduction

Electroweak (EW) vector-boson scattering (VBS) is among the most interesting classes of processes first accessible at the LHC to investigate the EW gauge structure and EW symmetry breaking. Taking into account leptonic decays of the EW gauge bosons, the experimental signature of VBS at the LHC is given by two mostly forward/backward-pointing jets and four leptons, with at least two of them charged and the others being neutrinos leading to missing transverse energy in the detector. The corresponding  $2 \rightarrow 6$  matrix elements do not only involve purely EW diagrams, but also gluon exchange or even gluon-fusion channels, leading to a large number of partonic channels and a whole tower of next-to-leading order (NLO) corrections featuring not only pure QCD and EW corrections but also QCD–EW mixed contributions. Precision calculations for VBS processes have been continuously extended and refined over the last few decades and culminated in the knowledge of the full towers of NLO corrections for all relevant VBS processes at the LHC and the matching of fixed-order predictions with QCD parton showers (see Ref. [1] and references therein). The NLO corrections of all VBS processes share the feature that the EW channels, whose relative contribution is enhanced by dedicated VBS selection cuts, receive particularly large EW corrections of 10–15%.

In this article we summarize the salient features and results of a recent recalculation [2] of the NLO corrections to like-sign WW scattering. Previous results on QCD corrections [3, 4] including parton-shower matching [5] as well as on all NLO orders including pure EW and QCD–EW contributions [6] have been presented in the literature before. Apart from providing cross-checks to existing results, we also present an approximation of the NLO corrections based on gauge-invariant subcontributions featuring the VBS subprocess and on resonance expansions for the W-boson decays, as well as a detailed discussion of the so-called *effective vector-boson approximation* for leading-order (LO) predictions based on the picture of massive vector bosons as partons of the proton.

## 2. Like-sign W-boson scattering at NLO

Like-sign WW production at the LHC has the signature of two like-sign leptons, two jets, which are typically forward/backward pointing, and missing transverse momentum carried away by two neutrinos. For definiteness, we consider the process  $pp \rightarrow e^+ \nu_e \mu^+ \nu_\mu jj + X$ . The LO cross section for  $W^\pm W^\pm$  scattering receives contributions from  $qq$ ,  $q\bar{q}$ , and  $\bar{q}q$  partonic channels involving various (anti)quark combinations with positive/negative net electric charge, i.e. at LO there are no partonic channels involving initial-state gluons. Denoting the EW and the strong coupling constants as  $e$  and  $g_s$ , respectively, the LO matrix elements scale like  $O(e^6)$  or  $O(g_s^2 e^4)$ ; the respective contributions to the LO matrix element are denoted  $\mathcal{M}_{e^6}$  and  $\mathcal{M}_{g_s^2 e^4}$  in the following. The structural diagram featuring the VBS subprocess, an EW background diagram as well as a diagram with gluon exchange are illustrated in Fig. 1. The different types of VBS subdiagrams contained in  $\mathcal{M}_{e^6}$  are shown in Fig. 2. Squaring the LO matrix element leads to three different perturbative orders, scaling like  $\alpha^6$ ,  $\alpha_s^2 \alpha^4$ , and  $\alpha_s \alpha^5$ . The latter interference contribution is numerically strongly suppressed due to its colour structure (which demands identical quark generations in the two quark chains) and due to the fact that forward- or backward-enhanced  $t/u$ -channel propagators are not further enhanced by squaring. At NLO, each of the LO matrix elements can receive EW and QCD corrections, i.e. there

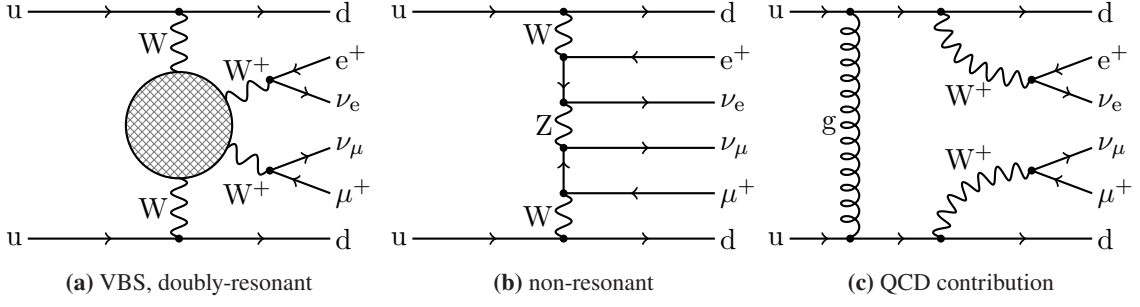


**Figure 1:** Examples of LO Feynman diagrams for the partonic subprocess  $uu \rightarrow dd e^+ \nu_e \mu^+ \nu_\mu$ . The shaded blob represents tree-level subdiagrams for  $W^+W^+ \rightarrow W^+W^+$ .

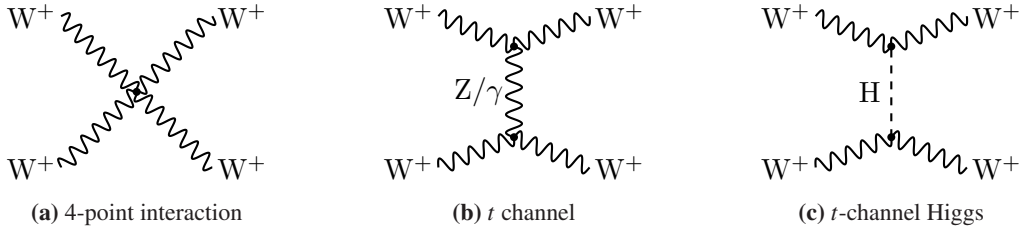


**Figure 2:** Typical VBS subdiagrams for  $W^+W^+ \rightarrow W^+W^+$  contained in the shaded blob of diagram Fig. 1a.

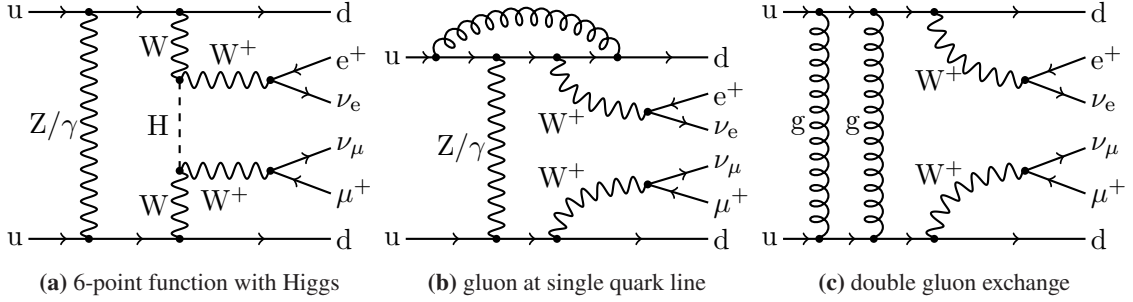


**Figure 3:** Examples of one-loop diagrams for the partonic subprocess  $uu \rightarrow dd e^+ \nu_e \mu^+ \nu_\mu$ .

are one-loop amplitudes of  $\mathcal{O}(e^8)$ ,  $\mathcal{O}(g_s^2 e^6)$ , and  $\mathcal{O}(g_s^4 e^4)$  at NLO. Some corresponding one-loop diagrams of these orders are shown in Fig. 3.

The cross sections are evaluated with the Monte Carlo program BONSAY, which is based on multi-channel Monte Carlo integration using adaptive weight optimization [7], similar to the approach described in Ref. [8]. BONSAY supports the parallel computation of uncertainties induced by different scale choices and errors in parton distribution functions. Both the tree-level and one-loop matrix elements are provided by OPENLOOPS2 [9] by default and have been cross-validated against respective results obtained with RECOLA [10]. The one-loop integrals are numerically evaluated using COLLIER [11], which employs the methods and results of Ref. [12] to numerically stabilize the results in the vicinity of exceptional phase-space configurations. Particle resonances are described in the complex-mass scheme [13, 14] to guarantee gauge independence of amplitudes and NLO accuracy in both resonant and non-resonant phase-space regions. The extraction and cancellation of (soft and collinear) infrared singularities is accomplished within the dipole subtraction formalism

both for QCD [15] and EW [16] corrections.

In addition to performing the full NLO calculation we have constructed a *VBS approximation (VBSA)* which can serve as a proxy for the full calculation with a precision that is sufficient for most phenomenological analyses and which is much less costly in terms of CPU time. At LO, the VBSA keeps the full  $2 \rightarrow 6$  matrix elements. At NLO, the VBSA merges two different approximative steps: Similar to the approach used in Ref. [4], step 1 selects all partonic channels that contain the VBS subprocess and further strips contributions of minor importance. In detail, matrix elements are decomposed into gauge-invariant parts characterized by different fermion-number flows, and only channels related to VBS are kept. This step, in particular, eliminates all channels featuring WWW production instead of VBS. Moreover, in the process of squaring the amplitude, all interference terms from different fermion-number flows are discarded, since they are colour suppressed and do not receive the kinematical VBS enhancements from squared  $t/u$ -channel W propagators. In step 1, thus, all one-loop amplitudes can be constructed from one prototype channel, e.g.  $cu \rightarrow e^+ \nu_e \mu^+ \nu_\mu ds$ , via crossing. Step 2 in the VBSA construction applies the *double-pole approximation (DPA)* to the produced W bosons in the virtual corrections, i.e. all one-loop matrix elements are expanded about the two W resonance poles. This procedure splits the virtual corrections into *factorizable* and *non-factorizable* parts, the former containing the corrections to the W-pair production and the W-decay subprocesses, the latter accounting for doubly-resonant effects from soft-photon exchange between the subprocesses. More details on the DPA concept and the specifically employed variant can be found in Refs. [14, 17, 18] and references therein. We finally note that care has to be taken in the approximation of the real-emission corrections since they are related to different underlying LO channels in different collinear limits of phase space. For the full construction of the VBSA we refer to Ref. [2].

### 3. Cross-section predictions at NLO

In Figs. 4–6 we compare the full relative NLO corrections  $\delta = d\sigma_{\text{NLO}}/d\sigma_{\text{LO}} - 1$  with its approximated version  $\delta_{\text{VBSA}} = d\sigma_{\text{NLO, VBSA}}/d\sigma_{\text{LO}} - 1$  in VBSA. The bands in the figures illustrate the residual scale uncertainties, obtained from the envelope of the usual seven-point scale variation with factors of 0.5 and 2 using the geometric mean of the transverse momenta of the tagging jets as central scale.

Figure 4 shows the results for the distributions in the transverse momenta of the leading jet and the positron. In both cases, for moderate and large  $p_T$ , the purely EW corrections of  $\mathcal{O}(\alpha^7)$  are dominant, negative, and increasing in magnitude for increasing transverse momenta, reaching about  $\sim -20\%$  and  $\sim -30\%$  at  $p_T = 600 \text{ GeV}$ , respectively. This behaviour is a typical sign for the appearance of EW Sudakov logarithms at high energies. The different size of the effects for jets and W-decay leptons can be understood as follows: The  $p_T$  distributions of the jets do not entirely zoom into the Sudakov regime of the  $WW \rightarrow WW$  subprocess, which demands large Mandelstam variables in the  $2 \rightarrow 2$  subprocess and small virtualities of the incoming (off-shell) W bosons. For large  $p_T$  values of a jet, the virtuality of at least one of the incoming W bosons is not small, and the  $t$ -channel momentum transfer in the  $WW \rightarrow WW$  subprocess is not forced to be large. Therefore, the EW Sudakov double logarithms cannot fully dominate the corrections to the  $p_T$  of the jets, and all kinds of nominally subleading EW high-energy corrections become relevant. On the other hand, the domain of large  $p_T$  of any of the decay leptons is dominated by the Sudakov

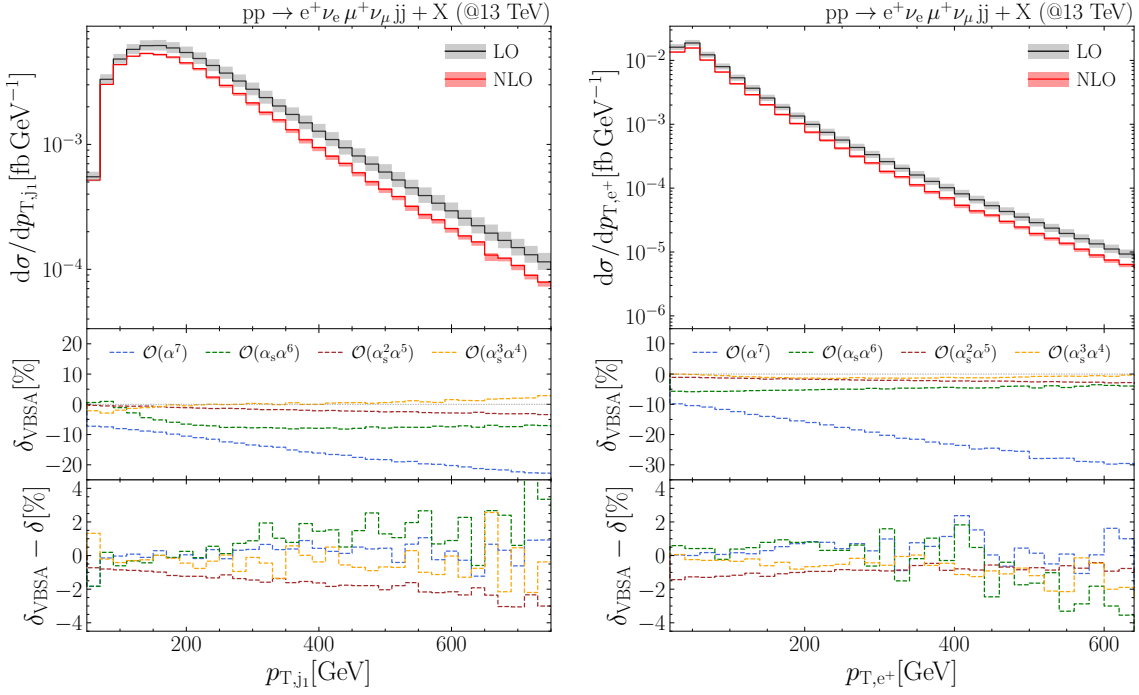


**Figure 4:** Distributions in the transverse momenta of the leading jet and the positron and corresponding corrections: absolute predictions (top panels), relative NLO corrections in VBSA (middle panels), and difference between relative full NLO corrections and corresponding VBSA (bottom panels). [Taken from Ref. [2].]

regime of the  $WW \rightarrow WW$  subprocess, because the preference of small jet transverse momenta leads to small virtualities of the incoming W bosons and the large transverse momentum of a decay lepton requires both a large scattering energy (Mandelstam variable  $s$ ) and large momentum transfer (Mandelstam variable  $t$ ) of the subprocess. The observed  $\sim -30\%$  can be qualitatively reproduced by just taking into account the EW Sudakov correction factor for the  $WW \rightarrow WW$  subprocess,  $\delta_{\text{Sud}} = -\frac{2\alpha}{\pi s_W^2} \ln^2(\hat{s}/M_W^2)$ , where  $\sqrt{\hat{s}} = \mathcal{O}(p_T)$  is the  $WW$  centre-of-mass energy and  $s_W$  the sine of the weak mixing angle. These features were already highlighted in Ref. [6]. The next-to-largest corrections to the  $p_T$  distributions are the mixed QCD–EW corrections of  $\mathcal{O}(\alpha_s \alpha^6)$ , which amount to 5–10% above the maximum in the leading-jet distribution and are almost uniformly  $\sim -5\%$  in the  $p_T$  spectrum of the electron. The suppression of the remaining corrections of  $\mathcal{O}(\alpha_s^2 \alpha^5)$  and  $\mathcal{O}(\alpha_s^3 \alpha^4)$  is mostly due to the fact that the cross-section contributions widely inherit the kinematic behaviour of the LO QCD contribution, which is small compared to the EW contribution over the whole distribution as a consequence of the VBS cuts. The approximative quality of the VBSA is typically at the 1% level for all orders of the NLO tower in the regions of phase space where the relevant part of the cross section is concentrated, with the exception of the  $\mathcal{O}(\alpha_s^2 \alpha^5)$  contribution where the difference  $\delta_{\text{VBSA}} - \delta$  can reach the order of 1.5% in size.

Figure 5 shows the distributions in the rapidities of the leading jet and the muon. The hierarchy among the various NLO contributions is similar as for the  $p_T$  distributions shown above, i.e. the purely EW corrections of  $\mathcal{O}(\alpha^7)$  are the dominating ones, followed by the order  $\mathcal{O}(\alpha_s \alpha^6)$ , while the other two orders with higher powers of  $\alpha_s$  are widely suppressed. The corrections of  $\mathcal{O}(\alpha^7)$

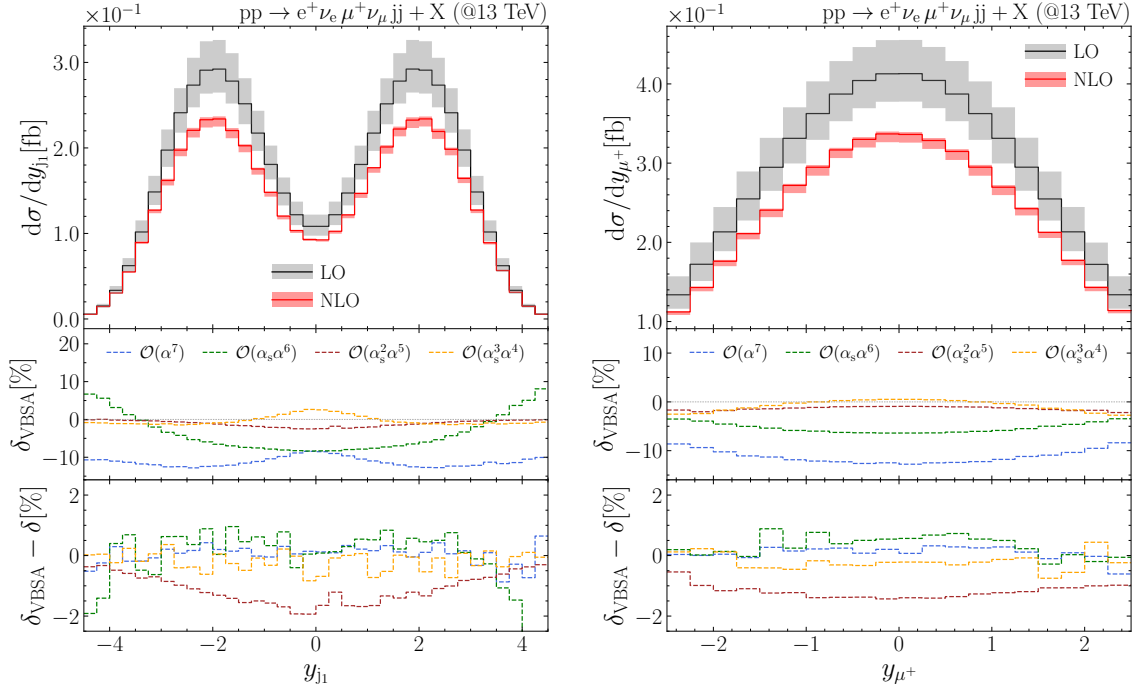


**Figure 5:** As in Fig. 4, but for the distributions in the rapidities of the leading jet and the muon. [Taken from Ref. [2].]

show much less variations in shape than for the  $p_T$  distributions and are typically about  $-10\%$  to  $-12\%$ . This is due to the fact that the large logarithmic EW high-energy corrections uniformly contribute to all rapidities, in contrast to the  $p_T$  distributions where they appear at high scales only. The moderate variations in the  $\mathcal{O}(\alpha^7)$  corrections mostly result from the change in the LO normalization induced by the variation in its composition from EW and QCD parts; normalizing the  $\mathcal{O}(\alpha^7)$  contribution to the  $\mathcal{O}(\alpha^6)$  LO part would produce a nearly flat relative  $\mathcal{O}(\alpha)$  correction. The overall second-largest corrections are again the ones of  $\mathcal{O}(\alpha_s \alpha^6)$ , which are dominated by the QCD corrections to the EW LO channel. Their largest impact, growing even to  $\sim 10\%$ , is on the leading jet at high rapidities. In the other rapidity regions those corrections hardly exceed  $5\%$ . The pure QCD corrections of  $\mathcal{O}(\alpha_s^3 \alpha^4)$  only exceed the  $1\%$  level significantly for central rapidities. The mixed corrections of order  $\mathcal{O}(\alpha_s^2 \alpha^5)$  never exceed the  $1\%$  level at all. Whenever the cross section is sizeable, the approximative quality of the VBSA is again at the level of  $1\%$  or better for all NLO orders but  $\mathcal{O}(\alpha_s^2 \alpha^5)$ , where it is of the order of  $1.5\%$ .

Finally, we show the distributions in the invariant mass of the two leading jets (left) and in the invariant mass of the charged leptons (right) in Fig. 6. The hierarchy of the various corrections and their behaviour can be widely explained following similar arguments as above. The trend of the dominating genuine weak corrections of  $\mathcal{O}(\alpha^7)$  towards increasingly negative corrections for larger scales is visible as for the  $p_T$  distributions, but the increase in size to about  $-15\%$  for the largest considered scales is much less dramatic. This is due to the fact that the domain of large invariant masses  $M_{j_1 j_2}$  or  $M_{e^+ \mu^+}$  is not fully dominated by the Sudakov regime of the  $WW \rightarrow WW$  subprocess, because the  $t/u$ -channel-like momentum transfer in the subprocess is not forced to be large. Thus,



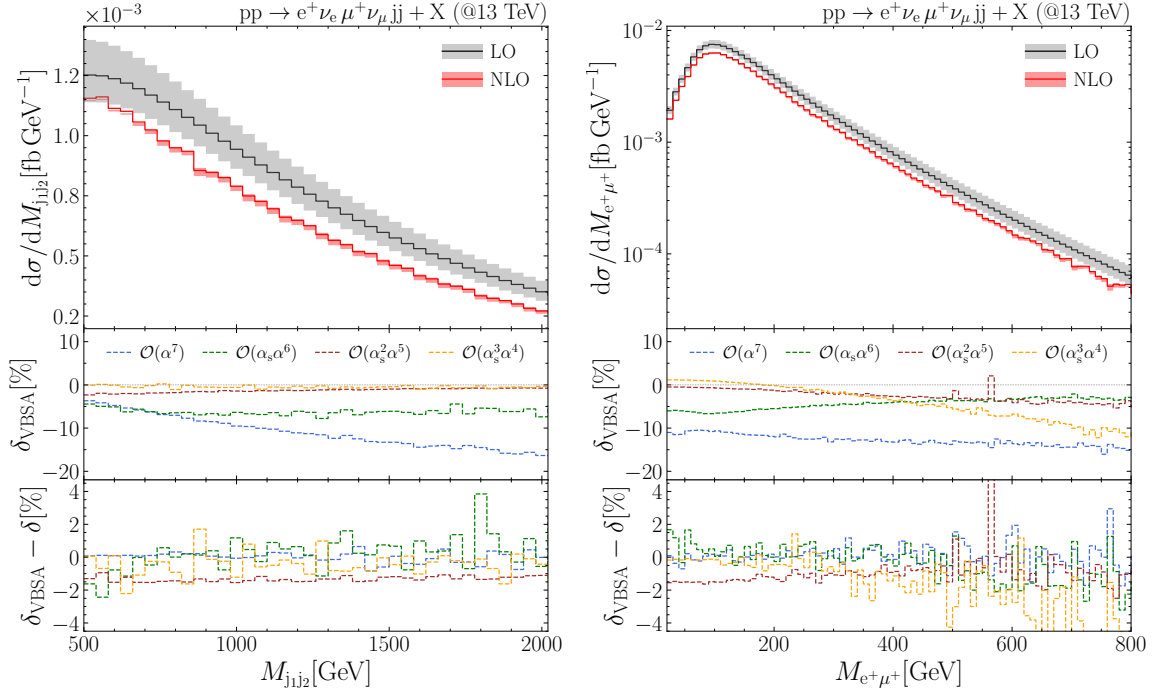


**Figure 6:** As in Fig. 4, but for the distributions in the jet-pair (left) and charged-lepton-pair (right). [Taken from Ref. [2].]

the impact of the leading EW Sudakov corrections is damped to the size of the subleading EW high-energy corrections. In the  $M_{j_{1j_2}}$  distribution, which is mostly dominated by EW contributions at LO, the corrections of  $\mathcal{O}(\alpha_s \alpha^6)$  typically have an impact at the 5% level, while the remaining two NLO orders with higher powers of  $\alpha_s$  hardly reach 1%. The mixed QCD–EW and the pure QCD corrections show, however, an interesting crossover in the  $M_{e^+\mu^+}$  distribution at  $M_{e^+\mu^+} \sim 400$  GeV, which we attribute to the increasing influence of the LO QCD contribution. For  $M_{e^+\mu^+} < 400$  GeV, where the EW part strongly dominates the LO cross section, the  $\mathcal{O}(\alpha_s \alpha^6)$  correction is the second largest after the genuine EW correction, and the remaining NLO orders are at the 1% level. For  $M_{e^+\mu^+} > 400$  GeV, where the LO QCD part competes in size with the EW LO part, the corrections of  $\mathcal{O}(\alpha_s^2 \alpha^5)$  and  $\mathcal{O}(\alpha_s^3 \alpha^4)$  dominate over  $\mathcal{O}(\alpha_s \alpha^6)$  and reach  $\sim -5\%$  for large  $M_{e^+\mu^+}$ . Similar to the previously considered distributions, the approximative quality of the VBSA is at the level of 1.5% for the  $\mathcal{O}(\alpha_s^2 \alpha^5)$  corrections and of 1% for the other NLO orders.

#### 4. Effective W-boson approximation at LO

The *effective vector-boson approximation (EVA)*, the idea of which goes back to Ref. [19], extends the idea of partons inside hadrons to the case of weak vector bosons, which play the role of partons in (anti)quarks, just like (anti)quarks and gluons in hadrons. The vector-boson emission  $q \rightarrow qV$  is approximated by its asymptotic behaviour in the collinear limit, where it is logarithmically enhanced. Previous studies in the literature have already indicated that the approximation quality of the EVA is rather limited (see, e.g., Refs. [20, 21] and references therein).

A comprehensive description of our construction of the LO EVA matrix elements is given

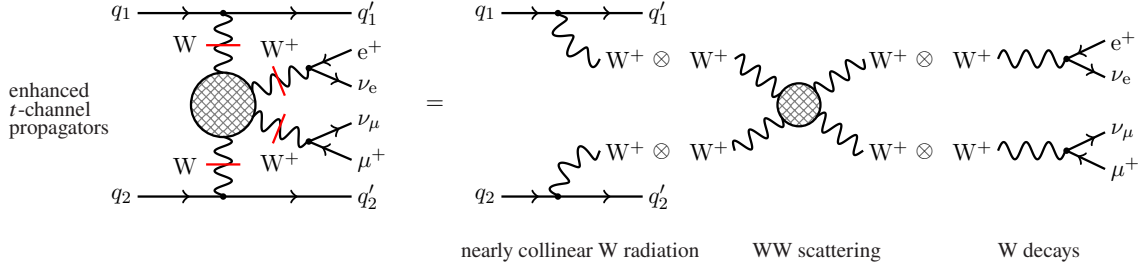


**Figure 7:** Schematic illustration of the EVA factorization of VBS matrix elements.

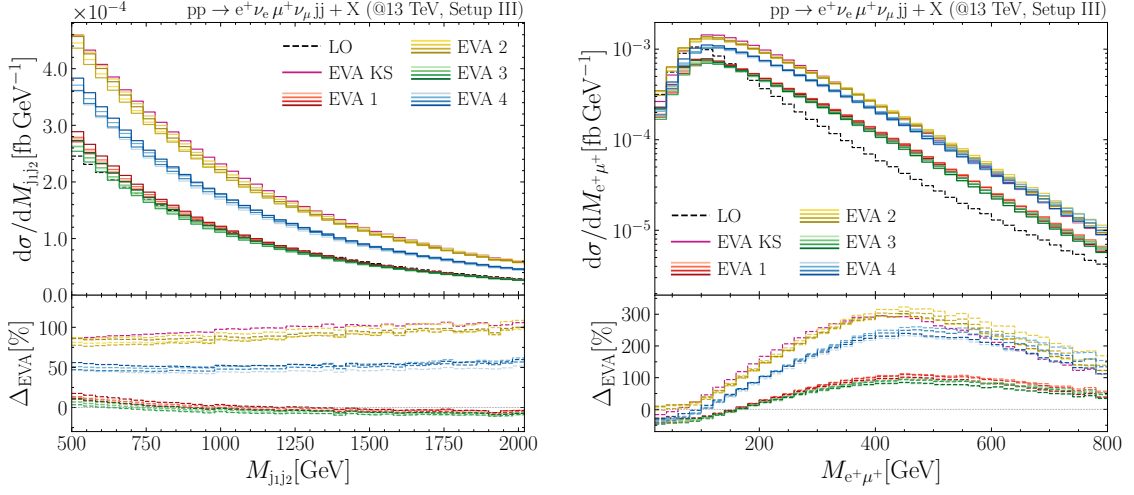


**Figure 8:** LO distributions in the invariant masses of the two jets and the two charged leptons, respectively, in like-sign WW scattering, based on full LO matrix elements (LO) and different EVA versions (EVA1–4 and EVA KS, see main text), employing typical VBS selection cuts but with an “inverted cut” on the jets transverse momenta,  $p_{T,\text{jet}} < 100$  GeV. The relative deviation of the EVA predictions from LO is quantified by  $\Delta_{\text{EVA}} = d\sigma_{\text{EVA}}/d\sigma_{\text{LO}} - 1$ . [Taken from Ref. [2].]

in the appendix of Ref. [2]. Figure 7 schematically illustrates the factorization of VBS matrix elements into W radiation off (anti)quarks, VBS core process, and subsequent W-boson decays. We do not merely take over existing proposals from the literature, but compare various formulations that differ in the details of handling intermediate (off-shell) polarization vectors and external currents describing the W radiation off the (anti)quarks and the W decays into leptons, in order to account for spin correlations and off-shell effects as much as possible.

Figure 8 exemplarily illustrates the quality of different EVA versions for the invariant-mass distributions of the two jets and the two charged leptons, respectively. More results can be found in Ref. [2]. The most important difference between the EVA versions is that EVA1 and EVA3 restore the transversality of the polarization vectors of initial-state W bosons in VBS amplitude, but not EVA2 and EVA4. Other, less important differences concern the transversality conditions for the final-state W bosons of the VBS process and for the leptonic decay currents, and an optional relative sign factor between transverse and longitudinal polarization vectors of the incoming (off-shell) W bosons, as described in detail in Ref. [2]. EVA KS refers to the EVA variant of Ref. [20],



where an extra weight factor was introduced for longitudinal incoming off-shell W bosons. All EVA versions are evaluated with an on-shell projection of the W momenta in the VBS subprocess that forces the W momenta on-shell to guarantee gauge independence of the  $WW \rightarrow WW$  matrix elements and preserves the locations of the photon poles in the  $t$ - and  $u$ -channel subdiagrams (b) of Fig. 2 to avoid extra enhancements in the intrinsic uncertainty of the EVA.

Generically, we find that all EVA versions can only qualitatively describe the full VBS process as long as typical VBS selection cuts are applied, which exclude the very forward region of jet emission for which the EVA is actually designed. Only if we invert the cut on the jets transverse momenta to  $p_{T,\text{jet}} < 100\text{--}150\text{ GeV}$ , the EVA delivers results of some reasonable approximative quality. In regions where the cross section is maximal, some EVA versions are good within 10–20% for distributions defined from the jet kinematics, but none are better than 50–100% for leptonic observables.

## 5. Conclusions

We have reported on a recent calculation [2] of the full tower of NLO corrections to like-sign W-boson scattering at the LHC, including all partonic channels and W-boson decays. Our calculation, which is implemented in the Monte Carlo integrator BONSAY, confirms the results of a previous calculation (up to a glitch in a numerically unimportant contribution) and in particular the occurrence of large pure EW corrections of the order of  $\sim -12\%$  for integrated cross sections.

Moreover, we have constructed a *VBS approximation* for the NLO prediction based on partonic channels and gauge-invariant (sub)matrix elements featuring the VBS subprocess and on resonance expansions of the W decays. The VBS approximation reproduces the full NLO predictions within  $\lesssim 1.5\%$  in the most important regions of phase space. Finally, we have discussed results from different versions of *effective vector-boson approximations* at LO, based on the collinear emission of W bosons of incoming (anti)quarks. In line with previous findings for similarly constructed approximations, we find that the approximative quality is only qualitative at the LHC owing to the mild collinear enhancement of the W-boson emission and the design of VBS analysis cuts, which excludes very forward/backward pointing jets.

## References

- [1] A. Ballestrero, *et al.* Eur. Phys. J. C **78** (2018) no.8, 671 [arXiv:1803.07943 [hep-ph]];  
R. Covarelli, M. Pellen and M. Zaro, Int. J. Mod. Phys. A **36** (2021) no.16, 2130009 [arXiv:2102.10991 [hep-ph]];  
D. Buarque Franzosi, *et al.* Rev. Phys. **8** (2022), 100071 [arXiv:2106.01393 [hep-ph]].
- [2] S. Dittmaier, *et al.* JHEP **11** (2023), 022 [arXiv:2308.16716 [hep-ph]].
- [3] B. Jäger, C. Oleari and D. Zeppenfeld, Phys. Rev. D **80** (2009), 034022 [arXiv:0907.0580 [hep-ph]];  
T. Melia, *et al.* JHEP **12** (2010), 053 [arXiv:1007.5313 [hep-ph]];  
F. Campanario, *et al.* Phys. Rev. D **89** (2014) no.5, 054009 [arXiv:1311.6738 [hep-ph]].
- [4] A. Denner, L. Hosekova and S. Kallweit, Phys. Rev. D **86** (2012), 114014 [arXiv:1209.2389 [hep-ph]].

- [5] B. Jäger and G. Zanderighi, *JHEP* **11** (2011), 055 [arXiv:1108.0864 [hep-ph]].
- [6] B. Biedermann, A. Denner and M. Pellen, *Phys. Rev. Lett.* **118** (2017) no.26, 261801 [arXiv:1611.02951 [hep-ph]]; *JHEP* **10** (2017), 124 [arXiv:1708.00268 [hep-ph]]; M. Chiesa, *et al.* *Eur. Phys. J. C* **79** (2019) no.9, 788 [arXiv:1906.01863 [hep-ph]].
- [7] F. A. Berends, R. Pittau and R. Kleiss, *Comput. Phys. Commun.* **85** (1995), 437-452 [arXiv:hep-ph/9409326]; *Comput. Phys. Commun.* **85** (1995), 437-452 [arXiv:hep-ph/9409326]; R. Kleiss and R. Pittau, *Comput. Phys. Commun.* **83** (1994), 141-146 [arXiv:hep-ph/9405257].
- [8] S. Dittmaier and M. Roth, *Nucl. Phys. B* **642** (2002), 307-343 [arXiv:hep-ph/0206070].
- [9] F. Cascioli, P. Maierhöfer and S. Pozzorini, *Phys. Rev. Lett.* **108** (2012), 111601 [arXiv:1111.5206 [hep-ph]]; F. Buccioni, *et al.* *Eur. Phys. J. C* **79** (2019) no.10, 866 [arXiv:1907.13071 [hep-ph]].
- [10] S. Actis, *et al.* *Comput. Phys. Commun.* **214** (2017), 140-173 [arXiv:1605.01090 [hep-ph]]; A. Denner, J. N. Lang and S. Uccirati, *Comput. Phys. Commun.* **224** (2018), 346-361 [arXiv:1711.07388 [hep-ph]].
- [11] A. Denner, S. Dittmaier and L. Hofer, *Comput. Phys. Commun.* **212** (2017), 220-238 [arXiv:1604.06792 [hep-ph]].
- [12] A. Denner and S. Dittmaier, *Nucl. Phys. B* **658** (2003), 175-202 [arXiv:hep-ph/0212259]; *Nucl. Phys. B* **734** (2006), 62-115 [arXiv:hep-ph/0509141]; *Nucl. Phys. B* **844** (2011), 199-242 [arXiv:1005.2076 [hep-ph]].
- [13] A. Denner, *et al.* *Nucl. Phys. B* **560** (1999), 33-65 [arXiv:hep-ph/9904472]; A. Denner, *et al.* *Nucl. Phys. B* **724** (2005), 247-294 [erratum: *Nucl. Phys. B* **854** (2012), 504-507] [arXiv:hep-ph/0505042].
- [14] A. Denner and S. Dittmaier, *Phys. Rept.* **864** (2020), 1-163 [arXiv:1912.06823 [hep-ph]].
- [15] S. Catani and M. H. Seymour, *Nucl. Phys. B* **485** (1997), 291-419 [erratum: *Nucl. Phys. B* **510** (1998), 503-504] [arXiv:hep-ph/9605323]; S. Catani, *et al.* *Nucl. Phys. B* **627** (2002), 189-265 [arXiv:hep-ph/0201036].
- [16] S. Dittmaier, *Nucl. Phys. B* **565** (2000), 69-122 [arXiv:hep-ph/9904440]; S. Dittmaier, A. Kabelschacht and T. Kasprzik, *Nucl. Phys. B* **800** (2008), 146-189 [arXiv:0802.1405 [hep-ph]].
- [17] A. Denner, *et al.* *Nucl. Phys. B* **587** (2000), 67-117 [arXiv:hep-ph/0006307].
- [18] S. Dittmaier and C. Schwan, *Eur. Phys. J. C* **76** (2016) no.3, 144 [arXiv:1511.01698 [hep-ph]].
- [19] S. Dawson, *Nucl. Phys. B* **249** (1985), 42-60; M. S. Chanowitz and M. K. Gaillard, *Phys. Lett. B* **142** (1984), 85-90; G. L. Kane, W. W. Repko and W. B. Rolnick, *Phys. Lett. B* **148** (1984), 367-372; J. Lindfors, *Z. Phys. C* **28** (1985), 427.
- [20] I. Kuss and H. Spiesberger, *Phys. Rev. D* **53** (1996), 6078-6093 [arXiv:hep-ph/9507204]; I. Kuss, *Phys. Rev. D* **55** (1997), 7165-7182 [arXiv:hep-ph/9608453].
- [21] E. Accomando, *et al.* *Phys. Rev. D* **74** (2006), 073010 [arXiv:hep-ph/0608019]; W. Bernreuther and L. Chen, *Phys. Rev. D* **93** (2016) no.5, 053018 [arXiv:1511.07706 [hep-ph]].